Cystine Uptake Inhibition Potentiates Front-Line Therapies In Acute Myeloid Leukemia

Bryann Pardieu, Justine Pasanisi, Frank Ling, Reinaldo Dal Bello, Justine Penneroux, Angela Su, Romane Joudinaud, Laureen Chat, Hsin Chieh Wu, Matthieu Duchmann, et al.

▶ **To cite this version:**

Bryann Pardieu, Justine Pasanisi, Frank Ling, Reinaldo Dal Bello, Justine Penneroux, et al.. Cystine Uptake Inhibition Potentiates Front-Line Therapies In Acute Myeloid Leukemia. Leukemia, 2022, 36 (6), pp.1585-1595. 10.1038/s41375-022-01573-6 . hal-04053984

HAL Id: hal-04053984
https://hal.science/hal-04053984v1

Submitted on 31 Mar 2023

HAL is a multi-disciplinary open access archive for the deposit and dissemination of scientific research documents, whether they are published or not. The documents may come from teaching and research institutions in France or abroad, or from public or private research centers.

L'archive ouverte pluridisciplinaire **HAL**, est destinée au dépôt et à la diffusion de documents scientifiques de niveau recherche, publiés ou non, émanant des établissements d'enseignement et de recherche français ou étrangers, des laboratoires publics ou privés.

CYSTINE UPTAKE INHIBITION POTENTIATES FRONT-LINE THERAPIES IN ACUTE MYELOID LEUKEMIA

AUTHORS: Bryann Pardieu[1], Justine Pasanisi[1], Frank Ling[1], Reinaldo Dal Bello[1,2], Justine Penneroux[1], Angela Su[1], Romane Joudinaud[1], Laureen Chat[1], Hsin Chieh Wu[1,3], Matthieu Duchmann[1], Gaetano Sodaro[1], Clémentine Chauvel[1,4], Florence A. Castelli[5], Loic Vasseur[1], Kim Pacchiardi[1,4], Yannis Belloucif[1], Marie-Charlotte Laiguillon[1], Eshwar Meduri[6], Camille Vaganay[1], Gabriela Alexe[7,8], Jeannig Berrou[9], Chaima Benaksas[1], Antoine Forget[1], Thorsten Braun[9], Claude Gardin[9], Emmanuel Raffoux[2], Emmanuelle Clappier[1,4], Lionel Adès[1,2], Hugues de Thé[1,3], François Fenaille[5], Brian J Huntly[6], Kimberly Stegmaier[7,8], Hervé Dombret[2,8], Nina Fenouille[1], Camille Lobry[1], Alexandre Puissant[1]*, Raphael Itzykson[1,2]*.

*equal contribution as senior co-authors. Electronic addresses:

alexandre.puissant@inserm.fr

raphael.itzykson@aphp.fr

AFFILIATIONS:

[1] Université de Paris, Génomes, biologie cellulaire et thérapeutique U944, INSERM, CNRS, F-75010 Paris, France;

[2] Département Hématologie et Immunologie, Hôpital Saint-Louis, Assistance Publique-Hôpitaux de Paris, F-75010 Paris, France;

[3] Collège de France, Oncologie Cellulaire et Moléculaire, PSL University, INSERM UMR1050, CNRS UMR 7241, Paris France;

[4] Laboratoire d'Hématologie, Hôpital Saint-Louis, Assistance Publique-Hôpitaux de Paris, F-75010 Paris, France ;

[5] Université Paris-Saclay, CEA, INRAE, Département Médicaments et Technologies pour la Santé (DMTS), MetaboHUB, F-91191 Gif-sur-Yvette, France;

[6] Wellcome Trust-Medical Research Council Cambridge Stem Cell Institute, Cambridge, UK;
[7] Department of Pediatric Oncology, Dana-Farber Cancer Institute and Boston Children's Hospital, Harvard Medical School, Boston, MA, USA;
[8] The Broad Institute of Harvard University and Massachusetts Institute of Technology, Cambridge, MA, USA;
[9] Université de Paris, Leukemia Transfer Lab, EA 3518, Institut de Recherche Saint-Louis, F-75010 Paris, France.

CORRESPONDENCE:
Raphael Itzykson
Service Hématologie Adultes, Hôpital Saint-Louis, 1 Avenue Claude Vellefaux, F-75010 Paris, France
Phone: +33 1 71 20 70 31
Fax: +33 1 42 38 51 28

KEYWORDS: Acute Myeloid Leukemia, Cysteine, Ferroptosis, Drug Repurposing.

Funding Sources. This study was funded by grants from Fédération Leucémie Espoir and Ligue Contre le Cancer, Comité Ile-de-France (RS18/75-15) to RI.

Running Head. Repurposing Sulfasalazine in AML.

This study has been presented in part at the 2021 Annual Meeting of the European Hematology Association.

Word Counts. Abstract: 197 words. Text: 3925 words. Figures: 5. Tables: 0. References: 58.

ABSTRACT

By querying metabolic pathways associated with leukemic stemness and survival in multiple AML datasets, we nominated *SLC7A11* encoding the xCT cystine importer as a putative AML dependency. Genetic and chemical inhibition of *SLC7A11* impaired the viability and clonogenic capacity of AML cell lines in a cysteine-dependent manner. Sulfasalazine, a broadly available drug with xCT inhibitory activity, had anti-leukemic activity against primary AML samples in *ex vivo* cultures. Multiple metabolic pathways were impacted upon xCT inhibition, resulting in depletion of glutathione pools in leukemic cells and oxidative stress-dependent cell death, only in part through ferroptosis.

Higher expression of cysteine metabolism genes and greater cystine dependency was noted in *NPM1*-mutated AMLs. Among eight anti-leukemic drugs, the anthracycline daunorubicin was identified as the top synergistic agent in combination with sulfasalazine *in vitro*. Addition of sulfasalazine at a clinically relevant concentration significantly augmented the anti-leukemic activity of a daunorubicin-cytarabine combination in a panel of 45 primary samples enriched in *NPM1*-mutated AML. These results were confirmed *in vivo* in a patient-derived xenograft model. Collectively, our results nominate cystine import as a druggable target in AML and raise the possibility to repurpose sulfasalazine for the treatment of AML, notably in combination with chemotherapy.

INTRODUCTION

Acute Myeloid Leukemias (AML) encompass a genetically heterogenous group of neoplasms with poor outcome.[1] Long-term survival remains limited with standard of care chemotherapies combining anthracyclines with cytarabine.[2] New therapies are needed to improve chemotherapy efficacy in AML. Resistance to chemotherapy frequently emerges from the expression of stemness-associated transcriptional programs.[3-5] Metabolic rewiring plays a prominent role in the drug resistance of leukemic cells.[6, 7] Targeting the metabolic vulnerabilities associated with stemness programs is thus an appealing approach in AML.[8, 9] Repurposing of clinically approved medicines is a promising approach in oncology, including in leukemias.[10, 11] We therefore sought to identify targetable metabolic vulnerabilities in AML correlated with stemness programs, focusing on the druggable genome.

By querying correlations between expression of stemness signatures and metabolic pathways in AML datasets, we identify expression of *SLC7A11* as a poor prognostic factor and a therapeutic target in AML. *SLC7A11* encodes the antiporter xCT that imports cystine, the oxidized dimer and main source of intracellular cysteine, and exports glutamate. Targeting xCT induced a ROS-dependent death caused by cystine depletion which was at least partially attributable to ferroptosis. Finally, we show that clinically relevant concentrations of sulfasalazine (SSZ), a drug approved for inflammatory diseases but known to competitively inhibit xCT activity,[12] can recapitulate this effect *in vitro* and *in vivo* and improve the activity of anthracycline-based chemotherapies in AML.

METHODS

Detailed methods are provided in the *Supplementary Appendix* available online.

Patient Derived Xenotransplants (PDX)

The French National committee on animal care reviewed and approved all mouse experiments described in this study. Sample sizes were chosen in light of the fact that these *in vivo* models were historically highly penetrant and consistent. Animals were excluded from the study if any signs of distress were observed without clinical signs of leukemia: absence of leukemic blasts in bone marrow, spleen, and blood. Blinded observers visually inspected mice for obvious signs of distress, such as loss of appetite, hunched posture, and lethargy. In a first experiment, 1 x10^6 *CEBPA*, *RUNX1*, *ASXL1*, *EZH2*, *TET2* and *JAK2* mutated primary AML cells were tail vein injected into 6 to 8 week-old sub-lethally irradiated recipient NSG-S (NSG-SGM3) males purchased from the Jackson Laboratory. This PDX model was chosen for its fast engraftment kinetics. Sixty days after injection, engraftment was confirmed by measuring circulating hCD45-positive blasts in blood (mean 0.8%±0.3%), and mice were randomized to receive SSZ at 400 mg/kg/12h IP for 30 days or vehicle (10% DMSO + 90% HBSS), according to previously published treatment regimens.[12, 13] Mice were euthanized after 30 days of treatment to evaluate leukemia burden in vehicle versus SSZ-treated groups. In a second experiment, 2.5 x 10^6 *FLT3*-ITD, *NPM1*c, DNMT3A^{R882H}, and IDH1^{R132H} AML primary cells (chosen for the presence of an *NPM1c* mutation) were tail vein injected into 10 to 12 week-old sub-lethally irradiated recipient NOD.Cg-Prkdcscid IL2rgtm1Sug Tg(SV40/HTLV-IL3, CSF2) 10-7Jic/Jic Tac (hu NOG-EXL) males purchased from Taconic. This mouse strain provided optimal engraftment for

this primary sample. Fifty days after injection, engraftment was confirmed as *supra* (mean hCD45^{+} blasts in blood 2.4%±1.3%). Following randomization, mice were treated once daily with chemotherapy (tail vein injection of 1mg/kg doxorubicin and 50mg/kg cytarabine for 3 days and intraperitoneal injection of 50mg/kg cytarabine for 2 additional days), twice daily with 150mg/kg SSZ (diluted in 10% DMSO + 90% HBSS) for 12 days, or both chemotherapy and SSZ. The '5+3' doxorubicin-based chemotherapy regimen was previously reported to mimic standard AML induction therapy.[14] Anthracycline dosing was reduced below the maximally tolerated dose and SSZ regimen lowered to allow concomitant administration. Bone marrow biopsies were performed on anesthetized animals at indicated time points. Sample were lysed in Red blood cell lysing buffer (Sigma-R7757), washed twice with PBS and resuspended in PBS 0.5%BSA (Sigma – A7906), 2mM EDTA prior to staining with APC-conjugated anti-human CD45 (BioLegend, 368512). Samples were washed 3 times before flow cytometry analysis. Mice were further followed-up for survival. No animals were excluded based on signs of distress in this experiment.

RESULTS

The cysteine biosynthesis pathway gene SLC7A11 is a poor prognostic factor in AML.

We first sought to determine through single-sample GSEA (ssGSEA) the metabolic pathways whose expression is positively correlated with stemness programs in two publicly available AML gene expression datasets (TCGA, GSE14468).[15, 16] In both cohorts, the cysteine/methionine biosynthesis pathway stood as the top metabolic pathway positively associated with expression of stemness programs, along with the branched-chain amino acid (valine, leucine and isoleucine) biosynthesis and lysine

degradation pathways (**Figure 1A-B** and **Supplementary Figure 1**). We next queried the metabolic dependencies of 12 AML cell lines with various genetic backgrounds, compared to 505 other cancer cell lines using the AVANA CRISPR library. This screen highlighted the specific functional dependency of AML cell lines on cysteine metabolism (**Figure 1C**). We therefore focused on cysteine metabolism pathway genes to identify those with prognostic relevance in AML patients. Our analysis uncovered a poor prognostic value for two genes, *CDO1* and *SLC7A11*, in both the TCGA and GSE14468 cohorts (**Figure 1D**). The poorer prognosis of AML patients expressing higher levels of *SLC7A11* which encodes the cystine/glutamate antiporter xCT was confirmed in a third cohort of 91 patients (GSE10358, **Figure 1E**).

Genetic and chemical inhibition of SLC7A11 has anti-leukemic activity

To address the potential relationship between the poorer clinical outcome observed in patients with high levels of *SLC7A11* and AML cell dependence on this target, we transduced three AML cell lines, IMS-M2, OCI-AML3, and MOLM-14 with multiple hairpins whose expression reduced SLC7A11 protein levels (**Figure 2A**). We observed a marked impairment in cell viability over a 6-day time course (**Figure 2B**). This effect was associated with a significant decrease in colony number of *SLC7A11*-depleted cells compared to those transduced with an empty vector control (**Figure 2C**). Of note, knockdown of *CDO1*, a gene downstream of *SLC7A11* in the cysteine metabolism pathway with an adverse prognostic value similar to *SLC7A11* (**Figure 1D**), did not decrease AML cell line viability (**Supplementary Figure 2**).

The *SLC7A11* gene product heterodimerizes with the promiscuous solute carrier heavy subunit encoded by *SLC3A2* to form a cystine-glutamate antiporter known as the xCT system.[17] Though the Alanine/Serine/Cysteine/Threonine (ASCT) neutral amino acid transporter encoded by *SLC1A4* can import cysteine from the extra-cellular environment, cystine import is the main source of intracellular cysteine, owing to the very limited amounts of reduced cysteine in the plasma.[18] Three chemically unrelated compounds have been previously reported to inhibit the activity of xCT, including erastin, (S)-4-Carboxyphenylglycine (CpG), and sulfasalazine (SSZ) [17]. SSZ is a broadly available medicine with a well-known, low toxicity profile and would thus be ideally suited for drug repurposing in AML.[19] We therefore tested the activity of these three xCT inhibitors in a panel of 20 cell lines encompassing a broad range of AML genetic backgrounds. Though their potency, as estimated by half-maximal inhibitory concentrations (IC_{50}), varied across cell lines, sub-millimolar activity was noted with both SSZ and CpG (**Figure 2D**) and to a lower extent with erastin (**Supplementary Figure 3**). To ascertain that the anti-leukemic activity of SSZ was due to xCT inhibition, we first compared dose-response curves of SSZ, CpG and erastin. Highly significant correlations were noted among the IC_{50}s of all three drugs (**Figure 2E**), suggesting that their anti-leukemic activity is caused by their shared xCT targeting mechanism, despite differences in their chemical structures and xCT-independent activities.[17] Of note, there was no clear correlation between total SLC7A11, SLC3A2 or ASCT expression by western blot and xCT dependence *in vitro* (**Supplementary Figure 4**). Neither of the two SSZ metabolites sulfapyridine and mesalazine, both of which lack xCT inhibitory activity,[12] inhibited the viability of the two cell lines most sensitive to SSZ (**Supplementary Figure 5**). Finally, given that the RPMI culture medium contains only cystine as an extracellular source of cysteine for cells, we sought to establish whether

supplementation with 1 mM cysteine of this cysteine-free culture medium counteracts the anti-leukemic effect of xCT inhibition by SSZ through ASCT-driven import of cysteine. Exogenous cysteine substantially alleviated response to SSZ of OCI-AML3 cells, confirming that SSZ affects primarily AML cell viability through the import of cystine and that this response can be rescued by transport of extracellular cysteine and subsequent oxidation to cystine (**Figure 2F**).

To critically assess the pre-clinical potential of SSZ in AML, we next examined the response to SSZ of twelve primary AML samples exhibiting various genetic alterations (Supplementary Table 5) and four $CD34^+$ specimens derived from healthy donors (**Figure 2G**). Consistent with our previous observation with cell lines, the twelve leukemia samples showed an enhanced sensitivity to SSZ treatment compared to the healthy donor derived $CD34^+$ cells (176 µM ± 40 µM versus 2.94 mM ± 4.21 mM, respectively, p=0.0011). *Ex vivo* treatment with SSZ of 6 primary AML samples impaired the long-term culture leukemic cell-initiating capacity, compared to vehicle (**Figure 2H**). Finally, *in vivo* administration of SSZ reduced the leukemic burden in a PDX model of AML (**Figure 2I**). Taken together, these studies indicate that targeting of cystine dependence either through SLC7A11 depletion or pharmacological xCT inhibition exhibits anti-leukemic activity in both human AML cell lines and primary patient specimens exposed to SSZ either in long-term culture or *in vivo*.

SCL7A11 expression is BRD4-dependent in AML

MYC-related transcriptional programs are important regulators of stem cell biology and regulate the self-renewal and survival of leukemic stem cells.[20] By querying various stemness-related transcriptional programs through ssGSEA, we found a significant

correlation between the activation of cysteine-methionine-related gene sets and multiple MYC-driven transcriptional signatures (**Figure 3A**). Bromo- and Extra-Terminal domain (BET) proteins, including BRD4, interact with acetylated histones in active regulatory domains (promoters and enhancers) and promote RNA Pol II activity. Despite the general nature of this mechanism, BET inhibitors such as OTX015, I-BET151, and JQ1, have been shown to have selective effects on gene expression through suppression of *MYC* and MYC-related transcriptional programs.[21, 22] Peaks corresponding to BRD4-binding regions and overlapping with the binding signal of the transcriptional activation histone mark H3K27Ac were present at the same promoter region of the human *SLC7A11* gene and at a putative super-enhancer in two independent ChIP-sequencing experiments performed in MOLM-14 and OCI-AML3 cells (**Figure 3B**). Other activation histone marks including H3K4me1 and H3K9ac were present at this region (**Supplementary Figure 6**), and CRISPRi-mediated repression of this super-enhancer confirmed its role in *SLC7A11* expression (**Figure 3C**). Consistent with its inhibitory effect on BET proteins, I-BET151 decreased the binding of BRD4 in these two regions, suggesting that BRD4 promotes the expression of *SLC7A11*. To test this hypothesis, we knocked down BRD4 in OCI-AML3 cells using two *BRD4*-directed shRNAs and observed a significant decrease in the expression of the canonical BRD4 transcriptional target *MYC* and *SLC7A11* both at RNA and protein levels (**Figures 3C and 3D**). Consistent with these results, the BET inhibitors, OTX015 and JQ1 reduced both *SLC7A11* mRNA and protein levels in the three AML cell lines tested (**Figures 3E and 3F**). Taken together, our results suggest that *SLC7A11* expression is substantially regulated by the BET protein BRD4.

xCT inhibition induces global metabolic rewiring and ROS-mediated cell death in AML

Clinically active drugs in AML impair leukemic viability by inducing apoptosis, cell cycle arrest and/or differentiation.[23] However, treatment of three different xCT-dependent AML cell lines with SSZ or CpG did not induce apoptosis as assessed by flow cytometry, caspase-3 cleavage, cell cycle arrest or differentiation (**Supplementary Figure 7**). In addition, electron microscopy in two cell lines revealed that treatment with SSZ did not induce morphological features of apoptosis or autophagy (**Supplementary Figure 8**). To gain insights into the metabolic consequences of xCT inhibition, we used a mass spectrometry-based metabolism profiling approach on IMS-M2 cells treated with either CpG or SSZ. Among 117 annotated metabolites, steady state levels of 38 (Supplementary Table 8) highly enriched in pathways directly coupled to cystine/cysteine metabolism, taurine and glutathione metabolism, as well as glycine, serine, and threonine metabolisms, or in pathways related to purine/pyrimidine, alanine/aspartate/glutamate, and glycerophospholipid metabolisms, were significantly altered upon xCT inhibition (**Figures 4A and 4B**).

Our analysis revealed a marked decrease in glutathione, one of the main products of the cystine/cysteine metabolism which exerts potent antioxidant activity by providing cellular protection against reactive oxygen species, ROS.[24, 25] Pronounced glutathione depletion upon xCT inhibition by CpG or SSZ was confirmed in IMS-M2 and OCI-AML3 cells (**Figure 4C**). According to this observation, SSZ triggered an accumulation of ROS as reflected by increased H2DCFDA intracellular fluorescence (**Figure 4D**). This effect was abolished by the two ROS scavengers, N-acetyl-cysteine (NAC) and 2-mercaptoethanol (2-ME, **Figure 4D**). In addition, NAC and 2-ME supplementation substantially decreased the sensitivity to SSZ and CPG of IMS-M2 and OCI-AML3 cells (**Figures 4E and 4F**). Of note, genetic invalidation of the ROS sensor *PML* did not alter the sensitivity of OCI-AML3 cells to SSZ (**Supplementary Figure 9**). Finally, using a

C11: BODIPY staining approach, we showed that SSZ-induced ROS accumulation promotes lipid peroxidation in IMS-M2, and, to a lesser extent, OCI-AML3 cells, an effect that was abrogated by NAC and 2-ME supplementation (**Figure 4G**). A peculiar form of cell death, known as ferroptosis, has been described as resulting from the accumulation of lipid-based ROS, particularly lipid hyperoxides. Given that this form of cell death is biochemically and morphologically distinct from other cell death modalities,[26] including apoptosis, necrosis, and necroptosis which are not induced by SSZ (**Supplementary Figure 7**), we investigated the effect of the ferroptosis inhibitor, ferrostatin-1, and showed this compound rescued partially the loss of viability induced by SSZ in IMS-M2 and OCI-AML3 cell lines (**Figure 4H**), as did the iron chelator deferoxamine, in contrast to inhibitors of apoptosis (QVD-OPH), autophagy (chloroquine) or necroptosis (necrostatin-1) (**Supplementary Figure 10**). Collectively these data show that xCT inhibition by SSZ in AML cells results in global metabolic rewiring and depletion of antioxidant defense systems including glutathione, resulting in ROS-dependent cell death.

Sulfasalazine synergizes with anthracycline-based chemotherapies in NPM1c AML

Among the panel of 20 AML cell lines tested for xCT dependency (**Figure 2D**), the two most sensitive to both SSZ and CpG were OCI-AML3 and IMS-M2, the only ones harboring *NPM1c* mutations. We therefore explored a possible specific dependency of *NPM1c* AMLs on xCT antiporter activity. Whereas NPM1c AMLs from both TCGA and GSE14468 exhibited comparable *SLC7A11* transcript levels (**Figure 5A**), they had higher expression of cysteine pathway genes (**Figure 5B**). In dose-response assays, OCI-AML3 and IMS-M2 required higher concentrations of cystine medium supplementation to rescue viability, compared to *NPM1* wildtype cell lines, suggesting

that NPM1c AML cell lines are more vulnerable to cystine import inhibition than their wild-type counterparts (**Figure 5C**). Of note, SSZ did not alter the cytoplasmic localization of the mutant NPM1c protein (**Supplementary Figure 11**).

Because of the trend towards greater xCT dependency in NPM1c AML, we performed dose-response viability assays in OCI-AML3 and IMS-M2 cells combining SSZ with a panel of 8 clinically available drugs all reported to have cytotoxic or differentiating activities in NPM1c AML (daunorubicin [DNR], cytarabine [AraC], actinomycinD [ActD], venetoclax [VEN]) or differentiating (arsenic trioxide [ATO], all-trans retinoic acid [ATRA], azacitidine [AZA] and selinexor [SEL]).[10, 11, 27-29] Synergism between SSZ and the anthracycline DNR was prominent in both cell lines (**Figure 5D**) and across all SSZ concentrations, including sub-micromolar (**Supplementary Figure 12**). Anthracyclines are administered in combination with AraC in AML. We thus leveraged a previously reported *ex vivo* drug sensitivity screen performed in 45 primary AML samples (including 38 *NPM1c* AMLs) by multiparametric flow cytometry after a 72-hour treatment in niche-like conditions.[30] Specifically, we explored the addition of a fixed, low concentration of SSZ (4 µM, in the range of trough plasma concentrations of SSZ)[31] to a 5-point 10-fold dilution of the DNR-AraC combination at a fixed 1:20 molar ratio mimicking conventional pharmacokinetics of these chemotherapeutic agents.[32] Overall, low SSZ concentration resulted in higher activity of the DNR-AraC combination on both the total leukemic bulk ($p<0.0001$) and on GPR56+ leukemic stem cells ($p=0.0006$, **Figure 5E**). To confirm the additive effect of SSZ on anthracycline-cytarabine chemotherapy combination *in vivo*, we transplanted primary leukemic blasts from a patient harboring NPM1c along with frequent NPM1c co-mutations (*DNMT3A*, *FLT3-ITD* and *IDH1*) into sub-lethally irradiated NOG-EXL recipient mice. Following engraftment, mice were randomly assigned to vehicle treatment, single-agent SSZ

(150 mg/kg twice daily) for two weeks, a maximally tolerated '5+3' regimen of doxorubicin (1 mg/kg/d for 3 days) and AraC (50 mg/kg/d for 5 days), or the combination of SSZ and Doxo-AraC chemotherapy (**Figure 5F**). Compared to vehicle-treated mice, single-agent SSZ significantly reduced leukemic burden in the bone marrow following treatment completion (**Figure 5G**). Importantly, the addition of SSZ to chemotherapy further reduced leukemic burden compared to chemotherapy alone, both at an early (**Figure 5G**) and a later time point following SSZ treatment completion (**Figure 5H**), and further expanded survival (**Figure 5I**).

Oxidative stress and anti-leukemic activity with clinical concentrations of sulfasalazine

In patients, orally administered SSZ is cleaved in the gut into 5-aminosalicylic acid and sulfapyridine. The SSZ pro-drug endowed with xCT inhibitory activity has limited plasma bioavailability, with peak concentrations of ~100 µM,[31] i.e. in the range of IC_{50} values of the most xCT-dependent cell lines (**Figure 2D**). We compassionately treated a patient with hyperleukocytic refractory AML with SSZ dosed in the lower range of regimens approved in adults (3-6 g/d). ROS induction was notable after 3 days SSZ exposure and increased at day 7 (**Figure 5J**), suggesting that SSZ-mediated SLC7A11 inhibition is clinically achievable. Addition of SSZ to a stably dosed palliative regimen of the cytoreductive agent hydroxyurea (HY) also resulted in a prompt, though transient, drop in the peripheral blood leukemic burden, allowing discontinuation of HY (**Figure 5K**). Collectively, these data confirm *in vivo* the single-agent anti-leukemic activity of SSZ, but also provide rationale for further clinical investigation of SSZ combination with anthracycline-based chemotherapies in AML.

DISCUSSION

Here we report a framework for the systematic interrogation of metabolic vulnerabilities amenable to drug repurposing in AML. By inspecting correlations between expression of metabolic pathway and stemness signatures in multiple datasets, we nominated the *SLC7A11* gene as a poor prognostic factor in AML. Genetic and chemical inhibition of its gene product, encoding the xCT cystine importer, reduced the viability of multiple AML cell lines and primary patient samples with diverse genetic backgrounds. Conversely, the poor prognostic value of higher *CDO1* expression was not associated to a functional dependency in two cell lines.

The BET protein BRD4 regulates key gene expression programs involved in leukemic progression, including those executed by the MYC oncogene.[21, 22] We found expression of the cysteine metabolism pathway to be closely related to MYC signatures in primary AML datasets. ChIP-Seq analyses revealed BRD4 binding at the *SLC7A11* promoter and putative enhancers, while genetic and chemical repression of BRD4 abrogated *SLC7A11* expression at both gene and protein levels. These findings are in keeping with the recent report of xCT downregulation upon BET protein degradation.[33] Thus, BRD4 appears to positively regulate the cysteine pathway through *SLC7A11* expression. Metabolic rewiring upon BET inhibition is increasingly recognized as an important mechanism of action and source of resistance to this drug class.[7] Further work is required to define the role of MYC itself in the regulation of *SLC7A11*.

In *SLC7A11*-dependent cell lines, chemical inhibition of xCT did not induce apoptosis, cell cycle arrest nor trigger differentiation. Unbiased metabolic profiling upon xCT inhibition revealed significant changes in multiple pathways, including in the anti-oxidant glutathione and taurine pathways.[24, 25] Glutathione levels were indeed reduced upon in vitro xCT inhibition, resulting in ROS induction. Addition of the ROS scavengers

NAC or 2-ME rescued viability upon xCT inhibition, demonstrating that xCT inhibition results in a form of ROS-dependent non-apoptotic cell death.

Impaired cystine import can trigger ferroptosis, a specific form of regulated cell death resulting from lipid peroxidation,[26] which has recently been studied in AML.[34] Though xCT inhibition in AML cell lines induced lipid peroxidation, the ferroptosis inhibitors ferrostatin-1 and deferoxamine only partly rescued cell viability upon xCT inhibition, suggesting that, beyond ferroptosis, other cell death mechanisms are triggered by ROS accumulation or glutathione depletion upon xCT inhibition in AML.[35, 36] Metabolic changes upon xCT inhibition were not limited to glutathione and taurine metabolism and included metabolites from the tricarboxylic acid cycle such as succinate or malate, and cystathionine, which is a precursor of cysteine but also of ketoglutaric acid.[37]

Conventional cell culture does not recapitulate human plasma concentrations of key metabolites,[38, 39] bone marrow oxygen tension,[40] or anti-oxidant defenses provided by the leukemic stroma.[33, 41] All of these limitations were taken in consideration in our niche-like culture conditions combining a stromal layer, physiological bone marrow oxygen tension (3%) and plasma-like medium,[30] limiting culture duration to 3 days, in keeping with other drug screening platforms for primary AML cells.[42, 43]

The ASCT cysteine transporter, which is expressed in AML cells, could provide resistance to xCT inhibition by allowing cysteine influx to compensate for cystine. However, concentrations of reduced cysteine are ~100 times lower than oxidized cystine in the human plasma.[18] The latter are within the ~100µM range, comparable to concentrations in conventional culture media, including our custom plasma-like medium (Supplementary Table 9).

Our study focused on SSZ as an xCT inhibitor because of its excellent safety profile and immediate availability for clinical trials.[19] SSZ is active in inflammatory diseases, possibly through inhibition of NFκB pathways.[44] Several lines of evidence nevertheless demonstrate that the anti-leukemic activity of SSZ results from xCT inhibition. The sensitivity profile of a panel of 20 AML cell lines to SSZ was highly correlated to that of other xCT inhibitors including CpG and erastin.[45, 46] This anti-leukemic activity was recapitulated by shRNA-mediated SLC7A11 repression and was rescued by cysteine.

The reduction in leukemic burden in 45 primary AML samples exposed to 4μM SSZ, a concentration within the range of SSZ trough concentrations in patients,[31] and the finding of ROS induction and cytoreduction in a clinical setting, provide evidence that xCT inhibition can be achieved in patients by oral administration of conventional SSZ dosing regimens. The therapeutic window for xCT inhibitors in AML is further supported by >10-fold increased sensitivity of primary AML samples to SSZ compared to healthy CD34+ cells.

NPM1c AML, the most frequent AML genetic group,[1] is exquisitely sensitive to oxidative stress, although the molecular underpinnings for this ROS vulnerability remain unclear.[11, 47] Despite indications that NPM1c could be a biomarker of xCT dependence, dose-response assays to single-agent SSZ revealed no difference between *NPM1* mutated and wild type primary samples and chemosensitization by SSZ was noted regardless of *NPM1* status (*not shown*).

Repurposing of SSZ to inhibit xCT has been investigated alone or with standard of care therapies in non-hematological malignancies, so far with mitigated results.[48-50] Novel agents in AML often require combination therapy to fulfill their anti-leukemic potential. We uncovered robust synergism between SSZ and the anthracycline daunorubicin

(DNR), possibly through anthracycline mediated ROS induction.[51, 52] In patients, anthracyclines are administered in combination with cytarabine, which did not synergize with SSZ. The clinical relevance of this finding was however confirmed by *in vitro* and *in vivo* experiments combining anthracyclines and cytarabine with or without SSZ, though doxorubicin had to be substituted for daunorubicin for *in vivo* experiments.[14]

A formal comparison between xCT inhibitors, which may affect cancer viability by multiple mechanisms,[53] more specific ferroptosis inducers such as GpX4 inhibitors,[54] and other GSH-depleting agents with promising anti-leukemic activity such as APR-246,[34] will be the focus of future studies. Our findings strengthen a growing interest in targeting cysteine metabolism in cancer cells,[55, 56] and prompt further investigation of novel, more specific xCT inhibitors in AML, all of which are still at very early stages of drug development.[57, 58] Until then, our findings support clinical investigation of xCT inhibition in combination with anthracycline-based chemotherapy in AML.

Acknowledgments. The authors thank Patrick Auberger and Didier Bouscary for helpful discussions, Jean-Michel Cayuela, Carole Albuquerque, Christophe Roumier, and Céline Decroocq from the Saint-Louis and Lille Tumor Banks for primary patient samples; Veronique Montcuquet, Nicolas Setterblad, Christelle Doliger, and Sophie Duchez from the Saint-Louis Research Institute Core Facility; Jean-Marc Massé and Alain Schmitt from the Electronic Microscopy Imaging Facility ('PIME') of Institut Cochin; and the technical staff from the DBA (Diagnostic Biologique Automatisé) platform of Saint-Louis Hospital. This work was also supported by the ATIP/AVENIR French research program (to A. Puissant), the EHA research grant for Non-Clinical Advanced Fellow (to A. Puissant), the Ligue Nationale Contre le Cancer (to A. Puissant), the Mairie de Paris Emergences grants (to A. Puissant), the INCA PLBIO program (PLBIO20-246, to A. Puissant), Fondation ARC (PGA1-RC20180206836 to R. Itzykson), Association Laurette Fugain (ALF2020-01 to R. Itzykson), Fondation Leucémie Espoir (to R. Itzykson), Ligue contre le Cancer – Comité Ile-de-France (RS18/75-15 to R. Itzykson), Association Princesse Margot (to R. Itzykson), and the US National Cancer Institute (NCI) (NIH R35 CA210030 to K. Stegmaier). A. Puissant is a recipient of support from the ERC Starting program (758848) and supported by the St Louis Association for Leukemia Research. This work was also supported by the Commissariat à l'Energie Atomique et aux Energies Alternatives and the MetaboHUB infrastructure (ANR-11-INBS-0010 grant to FC and FF).

Author contribution. RI and AP designed the study, performed analyses, and drafted the manuscript. HCW and HdT designed the PML-/- cell line. MCL, EM, BJH and CL performed and analyzed ChIP-Seq experiments. FC and FF performed metabolomic experiments and primary analyses. GA performed ssGSEA and AVANA dependency analyses under the supervision of KS. BP designed and performed all other

experiments with assistance from JP, FL, RdB, JP, AS, YB, RJ, LC, GS, CC, KP, CV, JB, CB, AF and NF. TB, CG, ER, LA and HD provided primary AML samples. LV MD and EC provided the molecular annotations for primary AML samples. All authors reviewed the manuscript and approved its final version.

Disclosures. The authors have no conflicts of interest to disclose. RI has consulted for Abbvie, Amgen, BMS/Celgene, Daiichi-Sankyo, Jazz Pharma, Karyopharm, Novartis and Stemline Therapeutics, and received research funding from Novartis and Janssen, none of which is related to the present work. KS has consulted for Kronos Bio, Auron Therapeutics, and Astra-Zeneca on unrelated topics, receives grant funding from Novartis which did not fund this project, and holds stock options with Auron Therapeutics on unrelated topics.

REFERENCES

1. Papaemmanuil E, Gerstung M, Bullinger L, Gaidzik VI, Paschka P, Roberts ND*, et al.* Genomic Classification and Prognosis in Acute Myeloid Leukemia. *N Engl J Med* 2016 Jun 09; **374**(23)**:** 2209-2221.

2. Dombret H, Gardin C. An update of current treatments for adult acute myeloid leukemia. *Blood* 2016 Jan 07; **127**(1)**:** 53-61.

3. Eppert K, Takenaka K, Lechman ER, Waldron L, Nilsson B, van Galen P*, et al.* Stem cell gene expression programs influence clinical outcome in human leukemia. *Nat Med* 2011 Aug 28; **17**(9)**:** 1086-1093.

4. Shlush LI, Mitchell A, Heisler L, Abelson S, Ng SWK, Trotman-Grant A*, et al.* Tracing the origins of relapse in acute myeloid leukaemia to stem cells. *Nature* 2017 Jul 06; **547**(7661)**:** 104-108.

5. Ng SW, Mitchell A, Kennedy JA, Chen WC, McLeod J, Ibrahimova N*, et al.* A 17-gene stemness score for rapid determination of risk in acute leukaemia. *Nature* 2016 Dec 15; **540**(7633)**:** 433-437.

6. Farge T, Saland E, de Toni F, Aroua N, Hosseini M, Perry R*, et al.* Chemotherapy-Resistant Human Acute Myeloid Leukemia Cells Are Not Enriched for Leukemic Stem Cells but Require Oxidative Metabolism. *Cancer Discov* 2017 Jul; **7**(7)**:** 716-735.

7. Su A, Ling F, Vaganay C, Sodaro G, Benaksas C, Dal Bello R*, et al.* The Folate Cycle Enzyme MTHFR Is a Critical Regulator of Cell Response to MYC-Targeting Therapies. *Cancer Discov* 2020 Dec; **10**(12)**:** 1894-1911.

8. Jones CL, Stevens BM, D'Alessandro A, Reisz JA, Culp-Hill R, Nemkov T*, et al.* Inhibition of Amino Acid Metabolism Selectively Targets Human Leukemia Stem Cells. *Cancer Cell* 2018 Nov 12; **34**(5)**:** 724-740 e724.

9. Pollyea DA, Stevens BM, Jones CL, Winters A, Pei S, Minhajuddin M*, et al.* Venetoclax with azacitidine disrupts energy metabolism and targets leukemia stem cells in patients with acute myeloid leukemia. *Nat Med* 2018 Dec; **24**(12)**:** 1859-1866.

10. Falini B, Brunetti L, Martelli MP. Dactinomycin in NPM1-Mutated Acute Myeloid Leukemia. *N Engl J Med* 2015 Sep 17; **373**(12)**:** 1180-1182.

11. El Hajj H, Dassouki Z, Berthier C, Raffoux E, Ades L, Legrand O*, et al.* Retinoic acid and arsenic trioxide trigger degradation of mutated NPM1, resulting in apoptosis of AML cells. *Blood* 2015 May 28; **125**(22)**:** 3447-3454.

12. Gout PW, Buckley AR, Simms CR, Bruchovsky N. Sulfasalazine, a potent suppressor of lymphoma growth by inhibition of the x(c)- cystine transporter: a new action for an old drug. *Leukemia* 2001 Oct; **15**(10)**:** 1633-1640.

13. Chung WJ, Lyons SA, Nelson GM, Hamza H, Gladson CL, Gillespie GY*, et al.* Inhibition of Cystine Uptake Disrupts the Growth of Primary Brain Tumors. *The Journal of Neuroscience* 2005; **25**(31)**:** 7101-7110.

14. Wunderlich M, Mizukawa B, Chou FS, Sexton C, Shrestha M, Saunthararajah Y*, et al.* AML cells are differentially sensitive to chemotherapy treatment in a human xenograft model. *Blood* 2013 Mar 21; **121**(12)**:** e90-97.

15. TCGA TCGAC. Genomic and epigenomic landscapes of adult de novo acute myeloid leukemia. *N Engl J Med* 2013 May 30; **368**(22)**:** 2059-2074.

16. Wouters BJ, Lowenberg B, Erpelinck-Verschueren CA, van Putten WL, Valk PJ, Delwel R. Double CEBPA mutations, but not single CEBPA mutations, define a subgroup of acute myeloid leukemia with a distinctive gene expression profile that is uniquely associated with a favorable outcome. *Blood* 2009 Mar 26; **113**(13)**:** 3088-3091.

17. Liu J, Xia X, Huang P. xCT: A Critical Molecule That Links Cancer Metabolism to Redox Signaling. *Mol Ther* 2020 Nov 4; **28**(11)**:** 2358-2366.

18. Fu X, Cate SA, Dominguez M, Osborn W, Özpolat T, Konkle BA*, et al.* Cysteine Disulfides (Cys-ss-X) as Sensitive Plasma Biomarkers of Oxidative Stress. *Scientific Reports* 2019 2019/01/14; **9**(1)**:** 115.

19. Chen J, Lin S, Liu C. Sulfasalazine for ankylosing spondylitis. *Cochrane Database Syst Rev* 2014 Nov 27; (11)**:** CD004800.

20. Yamashita M, Dellorusso PV, Olson OC, Passegue E. Dysregulated haematopoietic stem cell behaviour in myeloid leukaemogenesis. *Nat Rev Cancer* 2020 Jul; **20**(7)**:** 365-382.

21. Dawson MA, Prinjha RK, Dittmann A, Giotopoulos G, Bantscheff M, Chan WI*, et al.* Inhibition of BET recruitment to chromatin as an effective treatment for MLL-fusion leukaemia. *Nature* 2011 Oct 27; **478**(7370)**:** 529-533.

22. Zuber J, Shi J, Wang E, Rappaport AR, Herrmann H, Sison EA*, et al.* RNAi screen identifies Brd4 as a therapeutic target in acute myeloid leukaemia. *Nature* 2011 Oct 27; **478**(7370)**:** 524-528.

23. Carter JL, Hege K, Yang J, Kalpage HA, Su Y, Edwards H*, et al.* Targeting multiple signaling pathways: the new approach to acute myeloid leukemia therapy. *Signal Transduct Target Ther* 2020 Dec 18; **5**(1)**:** 288.

24. Schaffer SW, Azuma J, Mozaffari M. Role of antioxidant activity of taurine in diabetes. *Can J Physiol Pharmacol* 2009 Feb; **87**(2)**:** 91-99.

25. Muri J, Kopf M. Redox regulation of immunometabolism. *Nat Rev Immunol* 2020 Dec 18.

26. Stockwell BR, Friedmann Angeli JP, Bayir H, Bush AI, Conrad M, Dixon SJ*, et al.* Ferroptosis: A Regulated Cell Death Nexus Linking Metabolism, Redox Biology, and Disease. *Cell* 2017 Oct 5; **171**(2)**:** 273-285.

27. Balsat M, Renneville A, Thomas X, de Botton S, Caillot D, Marceau A*, et al.* Postinduction Minimal Residual Disease Predicts Outcome and Benefit From Allogeneic Stem Cell Transplantation in Acute Myeloid Leukemia With NPM1 Mutation: A Study by the Acute Leukemia French Association Group. *J Clin Oncol* 2017 Jan 10; **35**(2)**:** 185-193.

28. Brunetti L, Gundry MC, Sorcini D, Guzman AG, Huang YH, Ramabadran R*, et al.* Mutant NPM1 Maintains the Leukemic State through HOX Expression. *Cancer Cell* 2018 Sep 10; **34**(3)**:** 499-512 e499.

29. DiNardo CD, Tiong IS, Quaglieri A, MacRaild S, Loghavi S, Brown FC*, et al.* Molecular patterns of response and treatment failure after frontline venetoclax combinations in older patients with AML. *Blood* 2020 Mar 12; **135**(11)**:** 791-803.

30. Figueiras RDB, Pasanisi J, Joudinaud R, Duchmann M, Sodaro G, Chauvel C*, et al.* Niche-like Ex Vivo High Throughput (NEXT) Drug Screening Platform in Acute Myeloid Leukemia. *Blood* 2020; **136**(Supplement 1)**:** 12-13.

31. Yamasaki Y, Ieiri I, Kusuhara H, Sasaki T, Kimura M, Tabuchi H*, et al.* Pharmacogenetic characterization of sulfasalazine disposition based on NAT2 and ABCG2 (BCRP) gene polymorphisms in humans. *Clin Pharmacol Ther* 2008 Jul; **84**(1)**:** 95-103.

32. Lim WS, Tardi PG, Dos Santos N, Xie X, Fan M, Liboiron BD*, et al.* Leukemia-selective uptake and cytotoxicity of CPX-351, a synergistic fixed-ratio cytarabine:daunorubicin formulation, in bone marrow xenografts. *Leuk Res* 2010 Sep; **34**(9)**:** 1214-1223.

33. Piya S, Mu H, Bhattacharya S, Lorenzi PL, Davis RE, McQueen T*, et al.* BETP degradation simultaneously targets acute myelogenous leukemia stem cells and the microenvironment. *J Clin Invest* 2019 May 1; **129**(5)**:** 1878-1894.

34. Birsen R, Larrue C, Decroocq J, Johnson N, Guiraud N, Gotanegre M*, et al.* APR-246 induces early cell death by ferroptosis in acute myeloid leukemia. *Haematologica* 2021 Jan 7.

35. Dixon SJ, Stockwell BR. The role of iron and reactive oxygen species in cell death. *Nature Chemical Biology* 2014 2014/01/01; **10**(1)**:** 9-17.

36. Jones CL, Stevens BM, D'Alessandro A, Culp-Hill R, Reisz JA, Pei S*, et al.* Cysteine depletion targets leukemia stem cells through inhibition of electron transport complex II. *Blood* 2019 Jul 25; **134**(4)**:** 389-394.

37. Locasale JW. Serine, glycine and one-carbon units: cancer metabolism in full circle. *Nat Rev Cancer* 2013 Aug; **13**(8)**:** 572-583.

38. Cantor JR, Abu-Remaileh M, Kanarek N, Freinkman E, Gao X, Louissaint A, Jr.*, et al.* Physiologic Medium Rewires Cellular Metabolism and Reveals Uric Acid as an Endogenous Inhibitor of UMP Synthase. *Cell* 2017 Apr 06; **169**(2)**:** 258-272 e217.

39. Vande Voorde J, Ackermann T, Pfetzer N, Sumpton D, Mackay G, Kalna G*, et al.* Improving the metabolic fidelity of cancer models with a physiological cell culture medium. *Sci Adv* 2019 Jan; **5**(1)**:** eaau7314.

40. Spencer JA, Ferraro F, Roussakis E, Klein A, Wu J, Runnels JM*, et al.* Direct measurement of local oxygen concentration in the bone marrow of live animals. *Nature* 2014 Apr 10; **508**(7495)**:** 269-273.

41. Forte D, Garcia-Fernandez M, Sanchez-Aguilera A, Stavropoulou V, Fielding C, Martin-Perez D*, et al.* Bone Marrow Mesenchymal Stem Cells Support Acute Myeloid Leukemia Bioenergetics and Enhance Antioxidant Defense and Escape from Chemotherapy. *Cell Metab* 2020 Nov 3; **32**(5)**:** 829-843 e829.

42. Tyner JW, Tognon CE, Bottomly D, Wilmot B, Kurtz SE, Savage SL*, et al.* Functional genomic landscape of acute myeloid leukaemia. *Nature* 2018 Oct; **562**(7728)**:** 526-531.

43. Pemovska T, Kontro M, Yadav B, Edgren H, Eldfors S, Szwajda A*, et al.* Individualized systems medicine strategy to tailor treatments for patients with chemorefractory acute myeloid leukemia. *Cancer Discov* 2013 Dec; **3**(12)**:** 1416-1429.

44. Wahl C, Liptay S, Adler G, Schmid RM. Sulfasalazine: a potent and specific inhibitor of nuclear factor kappa B. *J Clin Invest* 1998 Mar 1; **101**(5)**:** 1163-1174.

45. Gasol E, Jiménez-Vidal M, Chillarón J, Zorzano A, Palacín M. Membrane topology of system xc- light subunit reveals a re-entrant loop with substrate-restricted accessibility. *The Journal of biological chemistry* 2004 Jul 23; **279**(30)**:** 31228-31236.

46. Dixon SJ, Patel DN, Welsch M, Skouta R, Lee ED, Hayano M*, et al.* Pharmacological inhibition of cystine-glutamate exchange induces endoplasmic reticulum stress and ferroptosis. *Elife* 2014 May 20; **3:** e02523.

47. Huang M, Thomas D, Li MX, Feng W, Chan SM, Majeti R*, et al.* Role of cysteine 288 in nucleophosmin cytoplasmic mutations: sensitization to toxicity induced by arsenic trioxide and bortezomib. *Leukemia* 2013 2013/10/01; **27**(10)**:** 1970-1980.

48. Robe PA, Martin DH, Nguyen-Khac MT, Artesi M, Deprez M, Albert A*, et al.* Early termination of ISRCTN45828668, a phase 1/2 prospective, randomized study of Sulfasalazine for the treatment of progressing malignant gliomas in adults. *BMC Cancer* 2009 2009/10/19; **9**(1)**:** 372.

49. Otsubo K, Nosaki K, Imamura CK, Ogata H, Fujita A, Sakata S*, et al.* Phase I study of salazosulfapyridine in combination with cisplatin and pemetrexed for advanced non-small-cell lung cancer. *Cancer Sci* 2017; **108**(9)**:** 1843-1849.

50. Shitara K, Doi T, Nagano O, Imamura CK, Ozeki T, Ishii Y*, et al.* Dose-escalation study for the targeting of CD44v+ cancer stem cells by sulfasalazine in patients with advanced gastric cancer (EPOC1205). *Gastric Cancer* 2017 2017/03/01; **20**(2)**:** 341-349.

51. Gewirtz DA. A critical evaluation of the mechanisms of action proposed for the antitumor effects of the anthracycline antibiotics adriamycin and daunorubicin. *Biochem Pharmacol* 1999 Apr 1; **57**(7)**:** 727-741.

52. Tadokoro T, Ikeda M, Ide T, Deguchi H, Ikeda S, Okabe K*, et al.* Mitochondria-dependent ferroptosis plays a pivotal role in doxorubicin cardiotoxicity. *JCI Insight* 2020 May 7; **5**(9).

53. Soula M, Weber RA, Zilka O, Alwaseem H, La K, Yen F*, et al.* Metabolic determinants of cancer cell sensitivity to canonical ferroptosis inducers. *Nature Chemical Biology* 2020 2020/12/01; **16**(12)**:** 1351-1360.

54. Yusuf RZ, Saez B, Sharda A, van Gastel N, Yu VWC, Baryawno N*, et al.* Aldehyde dehydrogenase 3a2 protects AML cells from oxidative death and the synthetic lethality of ferroptosis inducers. *Blood* 2020 Sep 10; **136**(11)**:** 1303-1316.

55. Badgley MA, Kremer DM, Maurer HC, DelGiorno KE, Lee HJ, Purohit V*, et al.* Cysteine depletion induces pancreatic tumor ferroptosis in mice. *Science* 2020 Apr 3; **368**(6486)**:** 85-89.

56. Hu K, Li K, Lv J, Feng J, Chen J, Wu H*, et al.* Suppression of the SLC7A11/glutathione axis causes synthetic lethality in KRAS-mutant lung adenocarcinoma. *The Journal of Clinical Investigation* 2020 04/01/; **130**(4)**:** 1752-1766.

57. Lanzardo S, Conti L, Rooke R, Ruiu R, Accart N, Bolli E*, et al.* Immunotargeting of Antigen xCT Attenuates Stem-like Cell Behavior and Metastatic Progression in Breast Cancer. *Cancer Res* 2016 Jan 1; **76**(1)**:** 62-72.

58. Zhang Y, Tan H, Daniels JD, Zandkarimi F, Liu H, Brown LM*, et al.* Imidazole Ketone Erastin Induces Ferroptosis and Slows Tumor Growth in a Mouse Lymphoma Model. *Cell Chemical Biology* 2019 2019/05/16/; **26**(5)**:** 623-633.e629.

FIGURE LEGENDS

Figure 1. The cysteine biosynthesis pathway gene *SLC7A11* is a poor prognostic factor in AML. A-B. Heatmaps of ssGSEA z-scores for selected stemness and metabolic pathway gene expression signatures (Supplementary Table 1) from (**A.**) the TCGA-LAML (n=179) and (**B.**) the GSE14468 (n=526) AML cohorts. **C.** Volcano plot of gene set enrichment analysis of 90 metabolic pathways (Supplementary Table 3) with CERES dependency as a metric in AML (n=12) vs non-AML (n=505) cancer cell lines from the AVANA 18Q4 CRISPR/Cas9 screen library. **D.** Log-transformed unadjusted p values of univariable Cox models inspecting the prognostic value of each gene from the cysteine/methionine pathway (Supplementary Table 2) as continuous variables in patients from the TCGA-LAML (n=149) and GSE14468 (n=522) AML cohorts with available overall survival data. **E.** Overall survival of patients according to SLC7A11 expression higher or lower than median values in the TCGA-LAML (n=149), GSE14468 (n=522) and GSE10358 (n = 91) AML cohorts, p values from univariable analyses (log-rank tests).

Figure 2. Genetic and chemical inhibition of SLC7A11 has anti-leukemic activity **A.** Western blot of SLC7A11 and vinculin in IMS-M2, OCI-AML3 and MOLM14 cell lines transduced with *SLC7A11* targeting shRNAs or empty vector. **B.** Viability assessed by CellTiterGlo at different time points after doxycycline induction in IMS-M2, OCI-AML3 and MOLM14 cell lines transduced with *SLC7A11* targeting or empty vector control. Mean ±SD of CellTiterGlo luminescence relative to day 0 (7 technical replicates). Statistical difference between control and each shRNA across all time points was inspected by two-way ANOVA. **C.** Number of colonies (relative to control) after plating of $0.5x10^3$ OCI-AML3 cells transduced with shRNAs targeting *SLC7A11*

or empty vector for 14 days in methylcellulose. Mean ± SD of 3 technical replicates. Unpaired t tests with Welch correction. **D.** IC_{50} of SSZ and CpG in a panel of 20 AML cell lines after 5 days of culture measured by the CellTiterGlo viability assay. **E.** Pairwise Pearson correlation coefficients r and resulting *p* values between the IC_{50}s of the 3 xCT inhibitors across the 20 AML cell lines panel. **F.** Number of colonies (relative to untreated control) after plating of $0.5x10^3$ OCI-AML3 cells cultured for 14 days in methylcellulose in the presence of SSZ at indicated concentrations or DMSO vehicle with (red) or without (black) addition of cysteine (100mM). Mean ±SD of 3 technical replicates. Unpaired t tests with Welch correction. **G.** IC_{50} of SSZ in a panel of 12 primary AML samples and CD34+ cells from 4 healthy donors after 3 days of culture measured by CellTiterGlo. The dashed line indicates the 0.25 mM concentration retained for the long-term culture limiting dilution assay. P value from a Mann-Whitney test. **H.** Long-term culture initiating cell frequency determined by a 3-week liquid culture in niche-like conditions (hTERT-MSC-GFP feeder, 3% O_2) in limiting dilution with 250 µM SSZ or DMSO vehicle in 6 primary AML samples. Wilcoxon matched-pairs signed rank test. Characteristics of primary AML samples are in Supplementary Table 5. **I.** Proportion of hCD45+ leukemic cells in the bone marrow of NSG-S mice engrafted with a PDX model of AML with *CEBPA*, *RUNX1*, *ASXL1*, *EZH2*, *TET2* and *JAK2* mutations euthanized after 30 days of treatment with SSZ (400 mg/kg/12h, IP) or vehicle. Mann-Whitney test. *p<0.05, **p<0.01, ***p<0.001.

Figure 3. SLC7A11 expression is BRD4 dependent in AML. A. Heatmap of ssGSEA z-scores for cysteine-methione pathway program as reference and multiple MYC expression signatures from MSigDB and KEGG databases in the GSE14468 AML cohort.[15] **B.** ChIP-Seq data at the *SLC7A11* locus for H3K27Ac in untreated OCI-AML3

and MOLM-14 cells, and for BRD4 after treatment with DMSO or with the I-BET151 BET inhibitor. Blue boxes indicate the position of sgRNAs for CRISPRi inhibition of the Super-Enhancer region **C.** *SLC7A11* expression determined by RQ-PCR in MOLM14 cells after CRISPRi inhibition of the Super-Enhancer region or control vector. Mean ±SD of 3 technical replicates. Unpaired t tests with Welch's correction. **D.** *BRD4*, *MYC* and *SLC7A11* expression levels determined by RQ-PCR in OCI-AML3, cells after 36-hour doxycycline induction of BRD4-targeting shRNAs or empty vector. Mean ±SD of 4 technical replicates. Unpaired t tests with Welch's correction. **E.** Western blot of SLC7A11 and vinculin in OCI-AML3 cells after 36-hour doxycycline induction of BRD4-targeting shRNAs or empty vector. **F.** *MYC* and *SLC7A11* expression level determined by RQ-PCR in OCI-AML3, IMS-M2 and MOLM14 cells after 48-hour treatment with 1 µM JQ1, OTX15 or vehicle. Mean ±SD of 4 technical replicates. Unpaired t tests with Welch's correction. **G.** Western blot of SLC7A11 and vinculin (loading control) in protein extracts from OCI-AML3, IMS-M2 and MOLM14 cells after 48-hour treatment with 1 µM JQ1, OTX15 or vehicle. P values are from unpaired t tests with Welch's correction of 4 technical replicates. ***p<0.001.

Figure 4. xCT inhibition induces global metabolic rewiring and ROS-mediated cell death. A-B. Heatmap (**A.**) and Pathway Impact by MetaboAnalyst (**B.**) of the top 38 deregulated metabolites by LC-HRMS metabolomics in IMS-M2 cells treated for 72 hours with SSZ or CpG at IC_{50} (115 µM and 34.93 µM respectively) or DMSO. Six technical replicates. Cut-off for this list of metabolites: abs [log_2 (FC)]=1, p-val < 0.05 **C.** Mean ±SD of glutathione levels by colorimetric assay in IMS-M2 and OCI-AML3 after a 72-hour treatment with half-maximal inhibitory concentrations of SSZ (115 µM and 110 µM respectively) or CpG (34.93 µM and 28.22 µM respectively) or DMSO.

Unpaired t tests with Welch's correction. **D.** Histogram plots of H2DCFDA staining of indicated cell lines after 72-hour treatment with DMSO vehicle, 250 µM SSZ alone or combined with 55 µM 2-mercaptoethanol (2-ME) or 2 mM N-acetylcysteine (NAC). Results are from one representative experiment of three independent replicates. **E-F.** Dose-response curves from CellTiter-Glo viability assays in increasing concentrations of (**E**) SSZ or (**F**) CpG in OCI-AML3 and IMS-M2 cells with or without 55 µM 2-mercaptoethanol or 2 mM N-acetylcysteine. **G.** Histogram plots of C11-BODIPY staining of indicated cell lines after 72-hour treatment with DMSO vehicle, 250 µM SSZ alone or combined with 55 µM 2-mercaptoethanol, 2 mM N-acetylcysteine, or 10 µM ferrostatin-1. Results from one representative of three independent replicates. **H.** Dose-response curves from CellTiter-Glo viability assays after 5-day culture with increasing concentrations of SSZ/CpG in OCI-AML3 and IMS-M2 cells, with or without 10 µM ferrostatin-1 (Fer-1).

Figure 5. Sulfasalazine synergizes with anthracycline-based chemotherapies in AML. A-B. *SLC7A11* gene expression (**A.**) and ssGSEA z-scores of the Cysteine Metabolism Pathway (**B.**) in patients with mutant or wildtype *NPM1* from the TCGA-LAML and GSE14468 datasets (n=173 and n=525 with available *NPM1* status, respectively). P values from Mann-Whitney tests. **C.** Half maximal effective concentration (EC_{50}) of cystine supplemented in dose-response assays (5-point 2-fold serial dilution) to cystine/cysteine-free RPM1 1640 medium. CellTiterGlo viability readout after 5 days culture in 10 AML cell lines, according to *NPM1c* status. P value from Mann Whitney test. **D.** Bliss synergy scores (mean ± SE) across the full combination metrics of SSZ with indicated drugs (daunorubicin [DNR], cytarabine [AraC], actinomycinD [ActD], venetoclax [VEN], arsenic trioxide [ATO], all-trans retinoic

acid [ATRA], azacitidine [AZA] and selinexor [SEL]) in OCI-AML3 and IMS-M2 cells. Positive Bliss scores indicate synergism and negative scores antagonism. **E.** Difference in activity of DNR-AraC combination at a fixed 1:20 ratio on the in a 5-point dose-response assay in niche-like conditions with addition of a fixed 4 µM concentration of SSZ compared to addition of SSZ vehicle (DMSO 0.1%). Activity is measured as the untruncated actual area over the curve of total leukemic bulk (viable CD19-/CD3-/CD45+ cells) and gated viable CD19-/CD3-/CD45+/GPR56+ leukemic stem cells (LSCs). P values from paired t tests. **F.** Scheme of the *in vivo* treatment of a PDX sample (harboring *NPM1c*, $FLT3^{ITD}$, $DNMT3A^{R88H}$ and $IDH1^{R132H}$ mutations) transplanted into sub-lethally irradiated NOG-EXL recipient mice with vehicle (n=4), chemotherapy (n=4, doxorubicin 1 mg/kg/d d1-3 and cytarabine 50 mg/kg/d d1-5), SSZ (n=8, 150 mg/kg bid, d0-14) or chemotherapy + SSZ (n=8). **G-H.** Proportion of hCD45+ leukemic cells in bone marrow aspirates performed at day 16 (**G.**) and day 29 (**H.**), hence 2 days and 15 days after the last SSZ or vehicle administration). Note that bone marrow aspiration was a technical failure at day 29 in one of 8 mice from the chemo only group and two of 8 mice from the chemo + SSZ group. P values from Mann-Whitney tests. **I.** Overall survival of the four mice groups since the first day of treatments. P values from log-rank tests. **J.** Histogram plot of H2DCFDA staining in PBMCs (>90% blasts) from patient SLS341 prior to (day 0), at day 3 (SSZ 1.5g thrice-daily) and 7 (SSZ 2g thrice-daily) of a compassionate SSZ treatment. **K.** Longitudinal monitoring of white blood cell (WBC) count (left axis) and dosing of compassionate SSZ and cytoreductive hydroxyurea (HY, both on right axis) in patient SLS341. Day 0 refers to the start of SSZ therapy.

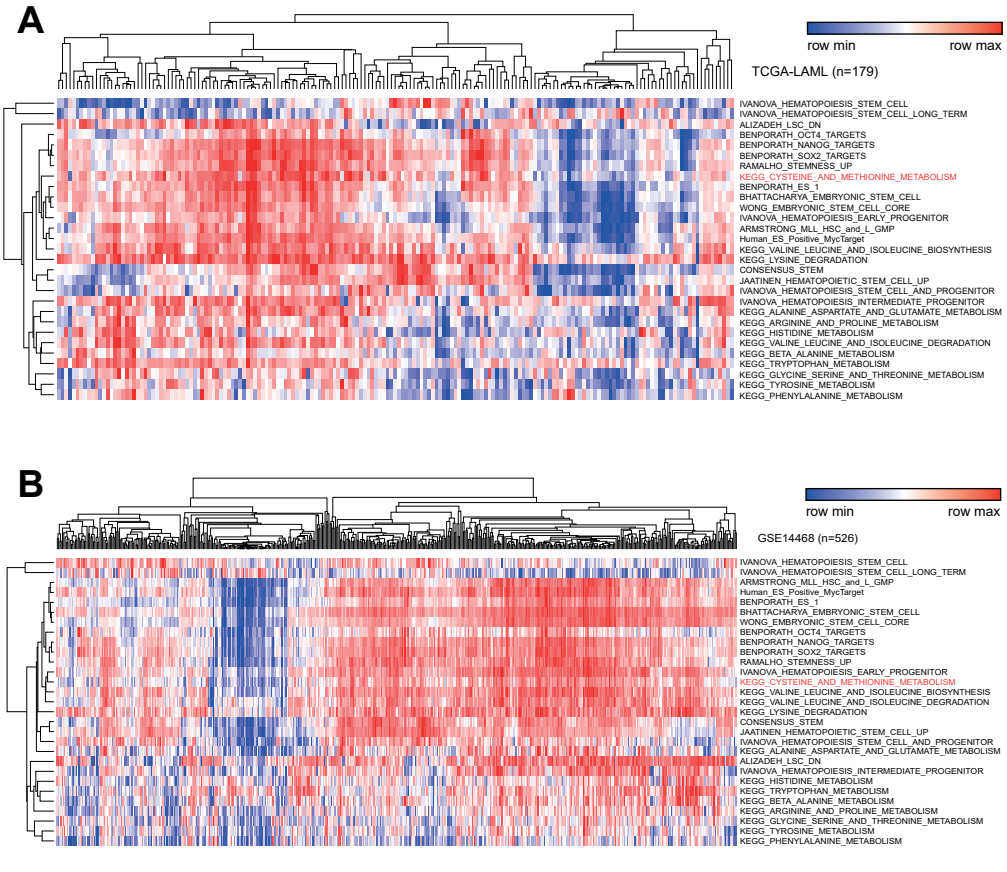

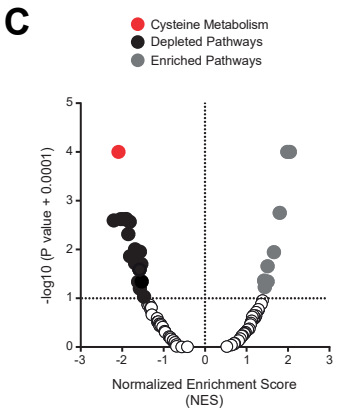

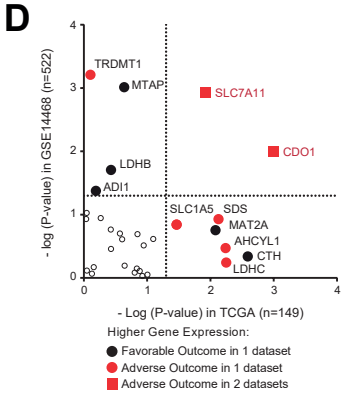

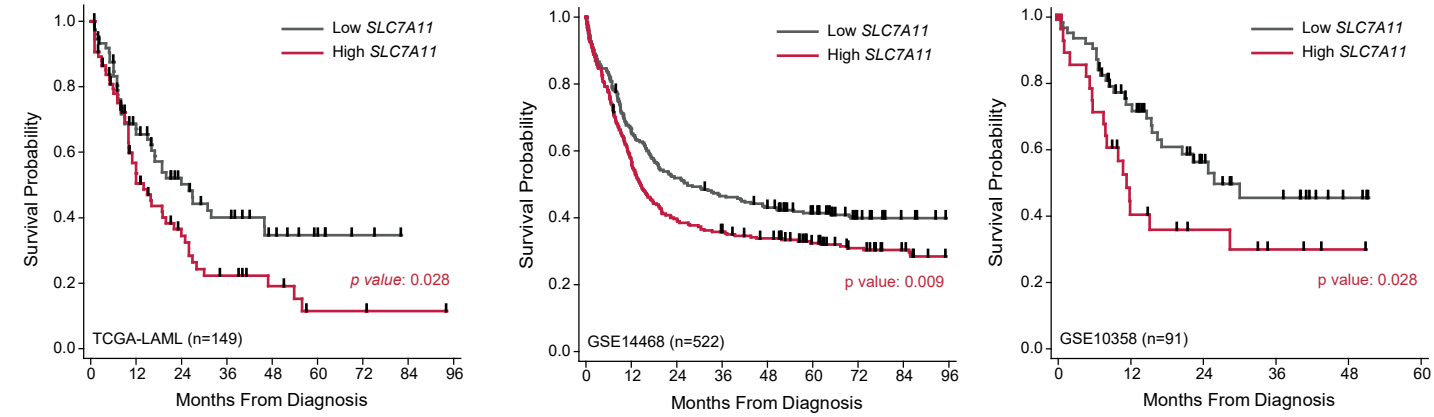

Pardieu et al. Figure 1

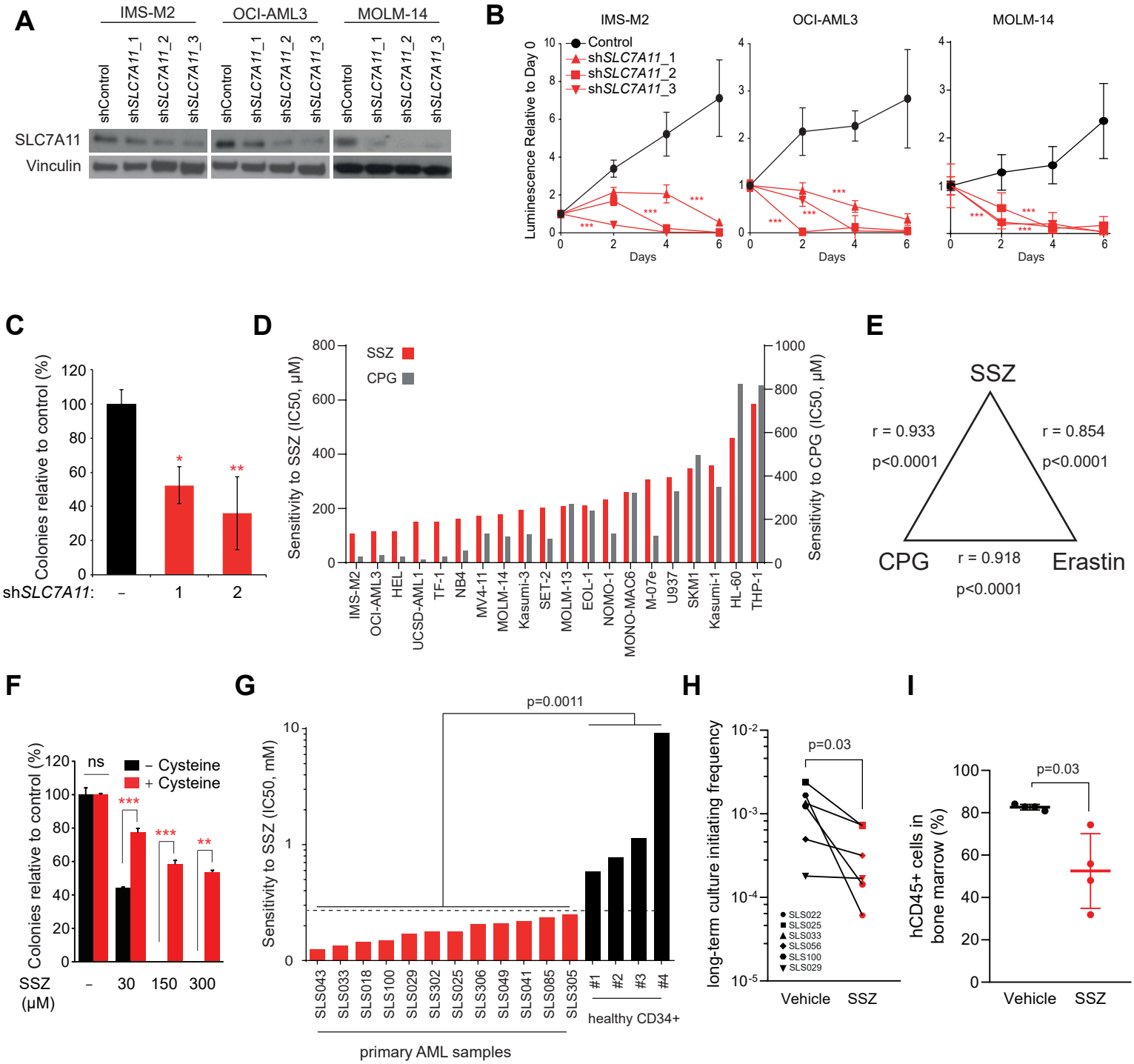

Pardieu et al. Figure 2

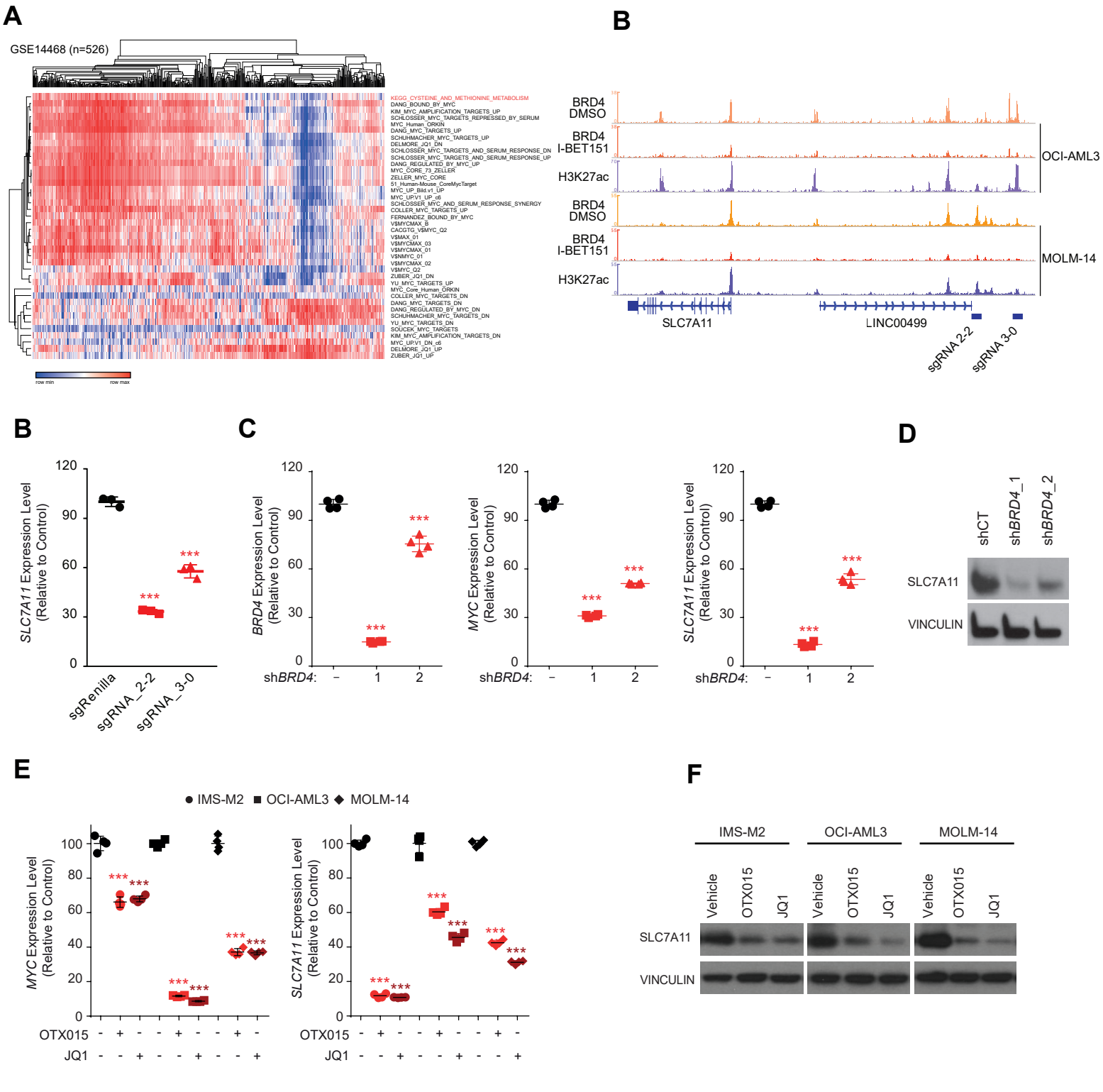

Pardieu et al. Figure 3

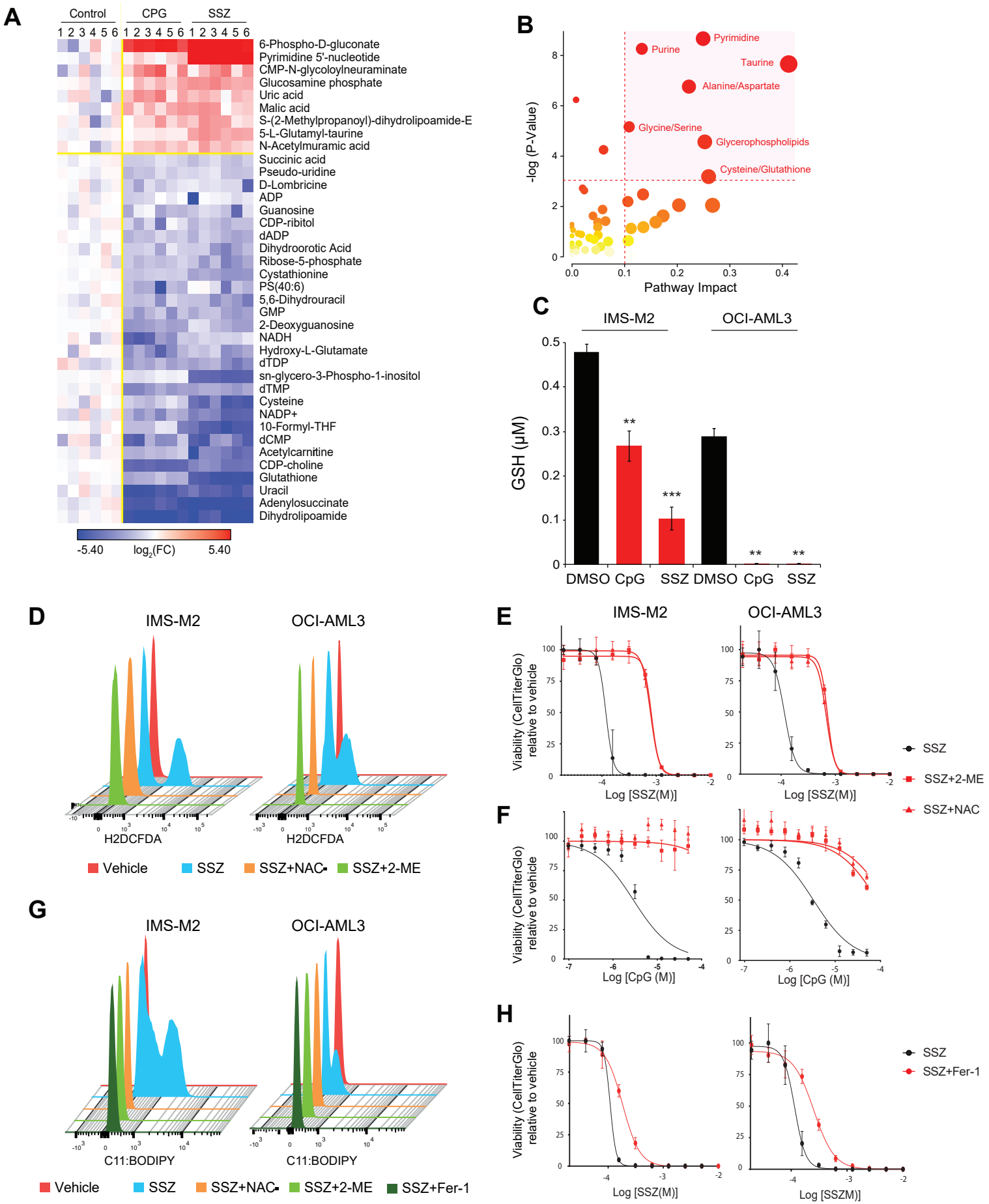

Pardieu et al. Figure 4

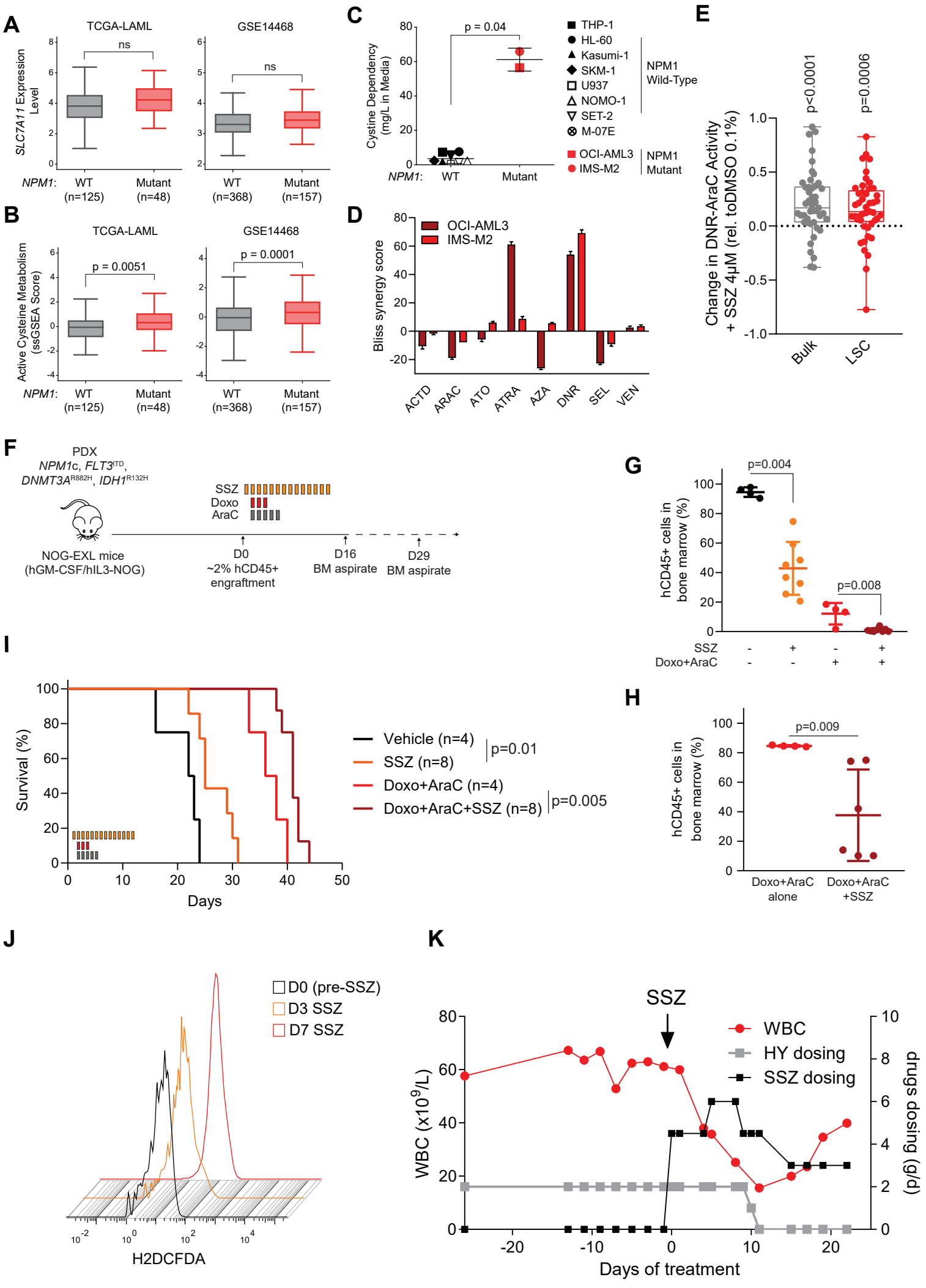

Pardieu et al. Figure 5